Biogenic Synthesis of Potassium-Doped Cobalt Oxide Nanoparticles and Tailoring the Effect on Structural, Optical, Electrical and Antimicrobial Properties

A. Ajitha[1], K. Seethalakshmi[2], S. Ravichandran[3,*], G. Ganesan Subramanian[4], C. Saravanan[5] and V. Jai Ganesh[6]

[1]Department of Physics, Tagore Institute of Engineering and Technology, Deviyakurichi-636112, Salem, Tamil Nadu

[2]Department of Physics, Sree Devi Kumari Women's College, Kuzithurai, Affiliated to Manonmaniam Sundaranar University, Abishekapatti, Tirunelveli - 627 012, Tamil Nadu

[3]Department of Chemistry, Tagore Institute of Engineering and Technology, Deviyakurichi-636112, Salem, Tamil Nadu

[4]Department of Electrical and Electronics Engineering, Tagore Institute of Engineering & Technology, Deviyakurichi, Salem, Tamil Nadu-636132 (India)

[5]Department of Physics, Tagore Institute of Engineering & Technology, Deviyakurichi, Thalaivasal(T.K), Salem(D.t), Tamil Nadu-636132

[6]Department of Mechanical Engineering, Tagore Institute of Engineering and Technology, Deviyakurichi, Salem, Tamil Nadu-636132

Abstract: Limited size effects and a high surface to volume ratio cause the features of nanoparticles to differ from those of the comparable bulk material. Alkali metal substitution has been found to improve the optical and electrical properties of pure Co_3O_4. Utilizing non-toxic, affordable, and environmentally favourable compounds is crucial for the production of nanoparticles. In order to create nanoparticles, a variety of metabolites from plant materials and animal products can be used. These metabolites can serve as fuel, capping agents, reducing agents, stabilizing or chelating agents for collecting metal ions. Thus Pure Co_3O_4 and K doped Co_3O_4 nanoparticles are created in the current study using an egg white-based microwave assisted hydrothermal method. Since egg albumen is an emerging biopolymer for creating biodegradable composites. By using different molar amounts of potassium [1, 3, and 5 mole%] as a dopant, we tried to improve the optical and electrical conductivity of cobalt oxide nanoparticles made from egg albumen, the natural biopolymer with green credentials using a microwave-assisted hydrothermal method. X-ray diffraction, energy dispersive X-ray spectroscopy, SEM analysis and dielectric studies were used to evaluate bare and doped samples. The found topology and small average crystallite size emphasize egg albumin's role as a stabilizer and size controller. Reduced optical band gap recommends using K doped samples for UV light absorption, which favours for optoelectronic device fabrication. Thus, by regulating K concentration, we may improve electrical conductivity and optical property of Co_3O_4 nanoparticles for device fabrication. The use of egg albumen and metal oxide (*i.e.*, cobalt oxide nanoparticles) in antibacterial applications are the primary focus.

Keywords: Egg albumen, Biopolymer, Microwave Assisted, Hydrothermal, Potassium dopant, Cobalt oxide.

INTRODUCTION

Multi-functional applications in physical science, biology, chemistry, medicine, and materials science have sparked a lot of curiosity with metal oxide nanoparticles. [Odiachi, I.J *et al*., 2023]. Cobalt oxide nanoparticles have received special attention due to their unique properties such as high chemical stability, catalysis, electrical conductivity, and antimicrobial activities, among others [Guoru Lie *et al*., 2022], [S Gopinath *et al*., 2022] [Luhan Wei *et al*., 2022]. Specifically, cobalt oxide, a semiconductor material has versatile applications including transparent conductive oxide, piezoelectric, photodetector, solar cell, photocatalyst antibacterial, gas sensor, etc. because of its direct wide band gap, non-toxicity, strong exciton binding energy, and high absorption in the ultraviolet (UV) region. When compared to chemical methods, green synthesis Co_3O_4's optical and electrical activity may open up new avenues in the device fabrication. Furthermore, the green synthesis of Co_3O_4 employing bio-reducing agents such as plants, fungi, bacteria, and yeast is more environmentally friendly and highly tuneable based on our need.

According to the relevant literature review, the generation of green synthesis nanoparticles with egg albumin assistance is rather uncommon. Because it is rapidly soluble in water and readily interacts with metal ions, egg white is well known for its capacity to froth and emulsify. Moreover, it serves as a gel or binder for materials used in moulding [P. Aji Udhaya and M. Meena., 2019]. The pure Co_3O_4 nanoparticles created

*Address correspondence to this author at the Department of Chemistry, Tagore Institute of Engineering and Technology, Deviyakurichi-636112, Salem, Tamil Nadu; E-mail: drravichandran.chemistry@tagoreiet.ac.in

Received on 26-05-2026 Accepted on 24-06-2026 Published on 02-07-2026

E-ISSN: 2311-8717/26

through green synthesis have very big particle sizes, according to different study reports. Cobalt oxide nanoparticles with a size range of 50 to 100 nm were created by Tahir Rasheed *et al*., 2019. The produced np's particle size ranged from 40 to 80 nm, according to Ismat Bibi *et al*., 2017. The 100 nm-sized cobalt oxide nps was made by Rajan Lakra *et al*., 2021.

It is advantageous to dope oxide compounds to improve their performance. Doping Co_3O_4 with metals and non-metals is the most effective technique to enhance its optical, electrical, magnetic, antibacterial, and photocatalytic capabilities. To boost electrical conductivity, doping elements were introduced to semiconducting materials [Yoo H *et al*., 2021]. According to various research findings, the potassium doped metal oxide nanoparticles have some advantages. To improve the catalytic characteristic, Batsile *et al*., 2107 synthesised potassium-doped Co_3O_4 nanoparticles. R Bhaviya *et al*., 2016. reported making ZnO nanoparticles with potassium as a dopant to enhance catalytic properties. For the purpose of controlling parasites, Overlay panel Yan Cao *et al*., 2021 produced K-doped ZnO nanoparticles. Po-Chih Chen and Sheng-Hsiung Yang, 2020., created potassium-doped nickel oxide to serve as the hole transit layer in steady and efficient inverted perovskite solar cells. Potassium-Doped Titanium Oxide Nanostructure was created by Lee, S.Y.*et al.* 2021 for enhanced photocatalytic activity. Potassium-Doped Zinc Oxide was made by Jie Bai *et al*., 2013, for use as a photocathode material in dye-sensitive solar cell uses. Potassium-doped Co_3O_4 catalyst for direct N_2O oxidation was revealed by Kimihiro Asano *et al*., 2008.

Metal oxide nanoparticle doping of alkali metals is quite uncommon. The inclusion of alkali promoters greatly improved the catalytic decomposition of NO over cobalt oxide. [P.W. Parka *et al*., 1998]. There were only a few researchers who combined alkali metals with metal oxides, including [Po-Chih Chen and Sheng-Hsiung Yang., 2019, Ai Serizawa., 2021, Jie Bai, Xiaobao Xu, *et al*]. A small number of researchers chose potassium as the doping agent for the cobalt oxide nanoparticles [Batsile M. Mogudi *et al*., 2017]. In a study published by Hongmei An *et al*. It has been discovered that potassium promotes the catalytic activity of transition metal oxides more strongly than other alkali metals.

Due to the aforementioned factors, we used a green technique with egg white to make cobalt oxide nanoparticles potassium as a dopant in a range of mole percentages. Our main objective is to investigate how altering the alkali metals (potassium) may impact the physical, optical, and electrical properties of the metal oxide (Co_3O_4) nanoparticles made utilising the green method of egg albumen a natural biopolymer. Reducing and stabilizing agent. Since, Natural polymers exhibit good intrinsic biocompatibility and enzymatic degradability, enabling intensive applications for biomedical applications [Abdelhamid and Hani Nasser., 2022]. In a study, it is said structural analysis by FTIR, XRD and SEM confirmed the incorporation of cobalt oxide nanoparticles in Gelatin/Polyethylene glycol/Chitosan (GPC) films, improved the mechanical strength, Flexibility, and thermal stability of the GPC films [Ali *et al*., 2025]. [Abd El-Aziz *et al*., 2025]

INSTRUMENTATION

Shimadzu's XRD diffractometer, monochromated with CuK radiation in the range of 10 to 80 ° at a 10 ° per minute scan rate, has been used to obtain PXRD patterns for calcined materials. Using the Jasco V-750 spectrophotometer, the UV-Vis Diffusion spectra were captured between 200 and 800 wavelengths. With the help of a field-emission scanning electron microscope, the structure morphology was studied (GEM-300, Carl Zeiss, Germany). Energy dispersive X-ray spectrometry with the Oxford Instruments X-Max was used to carry out the elemental study and the powdered materials were formed into pellets, and the AGILENT 4284 A was used to detect the dielectric parameters.

RESULTS AND DISCUSSION

Structural Characterization Using Xrd

For pure and doped samples, powder X-ray diffractogram analysis was done to look at crystallite size, crystallite structure, and lattice characteristics.

Figure **1** displays the K-doped and bare Co_3O_4 PXRD patterns that were observed. The diffraction peak at 2θ values of 31.21°, 36.9°, 38.55°, 44.9°, 55°,

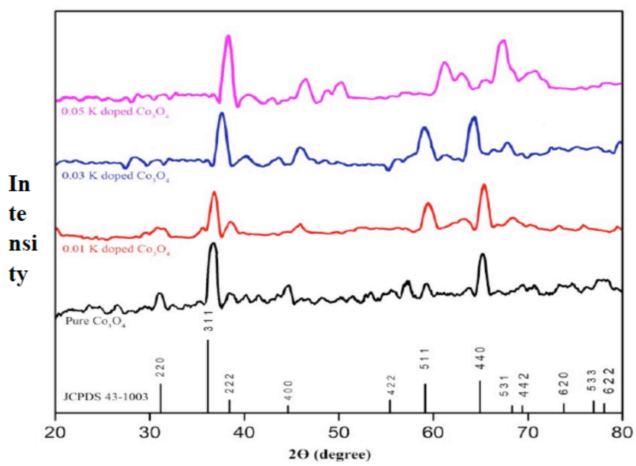

Figure 1: X-ray diffraction pattern for bare and K doped Co_3O_4 nanoparticles.

59.35°, 65.4°, 68.76°, 69.78°, 77.9°, and 78.38°, respectively, correspond to the standard pattern of face-centered cubic crystalline Co_3O_4 as per JCPDS card number (# 43-1003). The diffraction pattern shifts to a greater angle when potassium is present. There were no further peaks associated with the impurity phase with the increase in K concentrations, demonstrating that the phases are stable and K ions are equally integrated into the Co_3O_4 lattice. The intensity and crystallinity both decrease with a rise in doping concentration, possibly because of the strain created in the Co_3O_4 lattice as a result of the doping ion incorporation [Kalai Priya *et al*., 2020]. However egg albumen acts as a capping agent that reduces crystallite size, which broaden peaks and reduce intensity [Hmamouchi *et al*., 2022].

Using the Debye-Scherrer formula, the average crystallite size of the suggested samples was determined [M. Jothibas *et al*., 2023]. The lattice parameters were calculated using unit cell Win programme, and Table **1** includes a list of all calculated parameters along with the average crystallite size that was discovered.

With increasing concentration, the unit cell volume of K-doped Co_3O_4 decreased, illuminating the quantitative substitution of K ions in the lattice site. Dislocation density, which is correlated with the density of defects in the sample, is defined as the dimension of a dislocation per unit volume. Dislocation densities become abnormal as dopant concentrations rise [Trang Vu Thi *et al*., 2014]. Table **1** shows that the dislocation increases as K doping concentration rises, which suggests that K caused defects in the Co_3O_4 matrix and decreased crystallinity as a result of stress production and lattice contraction [Muslima Zahan & Jiban Podder., 2022]. The higher angle side of the potassium doped nanoparticles' XRD pattern experiences a slight peak shift as a result of changing lattice parameters [A. Kalai Priya.,2020]. Lattice characteristics including the lattice constant and crystallite size decrease as K dopant concentration rises, but strain and dislocation density also rise. Peak intensities were lower than in pure Co_3O_4, proving that potassium had been absorbed into the substance. The presence of egg albumen gives clear, sharp peaks of the crystals making eco-friendly nontoxic and biodegradable.

Bragg's law, which states that dopants cause an interplanar distance to decrease, can be used to explain this behaviour because cobalt (0.67Å) has a smaller ionic radius than potassium(1.33Å). After K doping, the diffraction peak intensities dropped, which showed a loss of crystallinity and an increase in surface defects in the samples. It is plausible to suppose that the doped sample may have greater electronic conductivity due to the aforementioned variables [Trang Vu Thi *et al*]. Metal doping should be utilised to modify the substance's average crystallite size, optical characteristics, and particle size in order to improve Co_3O_4's electrical and optical function. Lattice constants are slightly different from pure Co_3O_4.

SEM ANALYSIS

Figure **2** displays SEM micrographs of the processed samples. SEM analysis was used to examine the morphological properties of both the potassium-doped and unadorned cobalt oxide nanoparticles. SEM pictures show the size decrease of the nanoparticles. High-magnification SEM micrographs are used to examine all calcined Co_3O_4 nanoparticles, and they show that the tiny particles band together to form a structure resembling a bunch. As K concentration increases, the bunch-like shape alters, causing rough and denser structure to form. Clusters emerge, new phase formation with composite structures showing K doping increases the oxygen vacancies and surface adsorbed oxygen, altering surface roughness [Ao *et al*., 2025] illustrating that the strain develops as the concentration raise. Investigations using a scanning electron microscope

Table 1: Unit Cell Parameters Calculated from XRD & Particle Size from SEM Histogram

Sample	Pristine	1mol% K	3mol % K	5mol% K
Lattice parameter a (Å) (±0.01)	8.10	8.09	8.08	8.03
Volume V($Å^3$) (±1.8)	531.2	529.8	527.5	517.78
Average Crystallite size D(nm) (±0.03)	20.4	18.4	16.1	14.4
Average strain x 10^{-3} (± 0.5)	1.55	2.87	2. 93	3.81
Dislocation density x10^{-12} (±1.3)	2.39	2.94	3.84	4.81
Particle size D (nm) From SEM Histogram	24.2	21.6	18.6	15.2

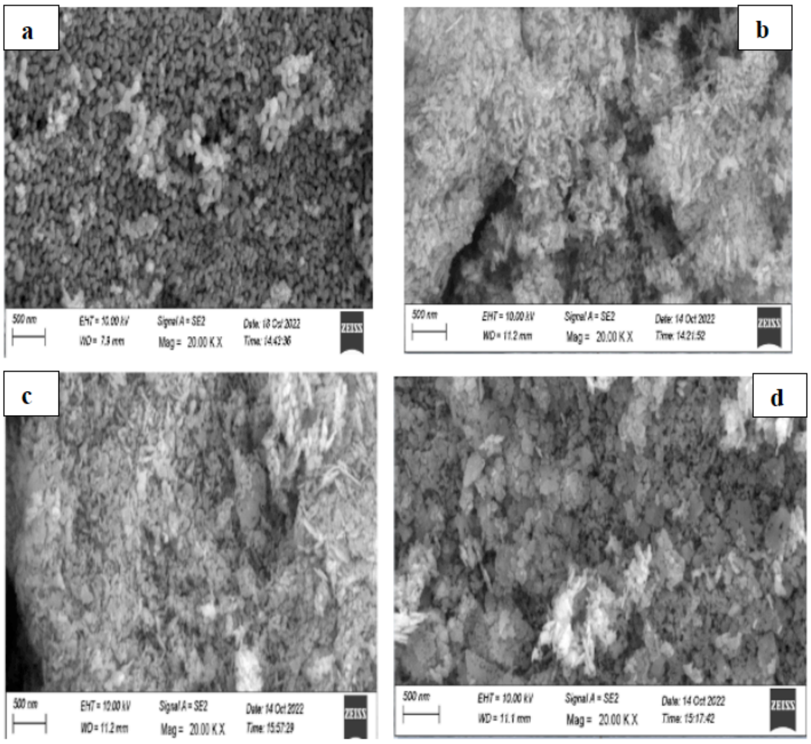

Figure 2: SEM images of **a)** Pure Co_3O_4 **b)** 0.01 K doped Co_3O_4 **c)** 0.03 K doped Co_3O_4 **d)** 0.05 K doped Co_3O_4.

(SEM) shows that the synthesised nanoparticles are crystalline.

PARTICLE SIZE DISTRIBUTION OF CO_3O_4 & K DOPED CO_3O_4

Particle size histograms for pure Co_3O_4 and altered with K are shown in Figure **3**. Figure **3** shows that as the potassium dopant concentration increases, the particle size of the grown nanoparticles decreases. This smaller, controlled particle is due to the presence of egg albumen [Chang *et al.*, 2026].

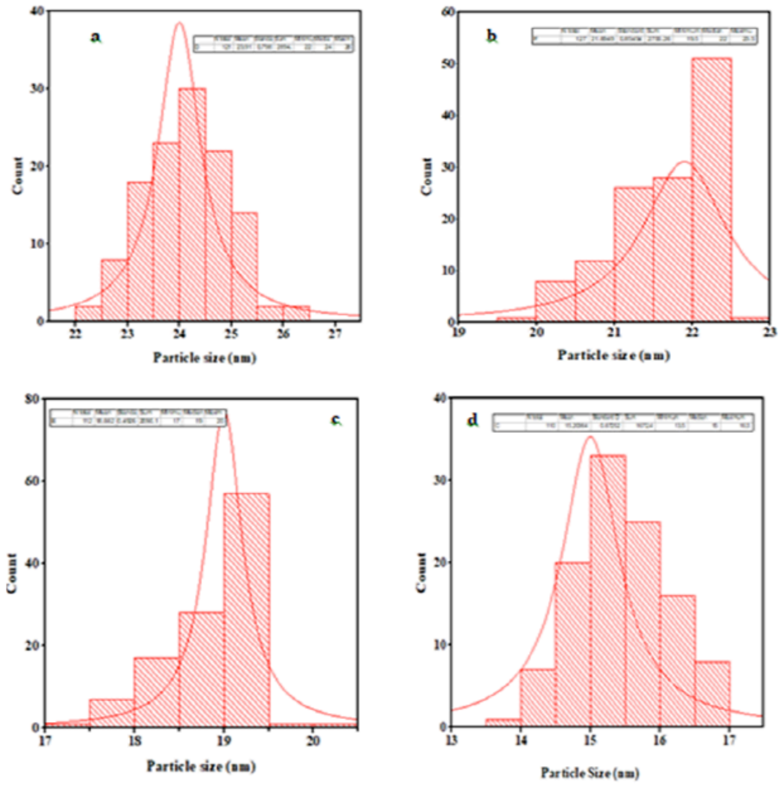

Figure 3: Particle size histogram of **a)** Pure Co_3O_4 **b)** 0.01 K doped Co_3O_4 **c)** 0.03 K doped Co_3O_4 **d)** 0.05 K doped Co_3O_4.

EDAX ANAYSIS

The spectra of cobalt oxide and K-enriched cobalt oxide nanoparticles are shown in Figure **4** for energy dispersive X-ray analysis. Chemical analysis spectra reveal prominent peaks associated with Co and O. According to the EDAX spectrum shown in Figure **4**, potassium is found with the elements Co and O. The purity of the sample may be determined by the efficient assembly of K into Co_3O_4 nanoparticles and the lack of other elemental peaks.

The purity of the samples is indicated by the elemental composition obtained by EDAX strictly showing the existence of cobalt and oxygen peaks alone for pure Co_3O_4 and K peaks additionally including in K doped Co_3O_4. The carbon tape employed as a support for FESEM imaging is responsible for the weak peak for C. The particles are uniformly covered with oxides, as seen in every photograph. The presence of cobalt may be seen in the peaks around 0.8 KeV, 7 KeV, and 7.9 KeV. The oxygen element is represented by the peak at almost 0.5 keV, while the potassium element is represented by the peak at almost 3.2 keV.

UV-DRS ANALYSIS

Using UV-DRS spectroscopy, the optical properties of the generated samples are examined. The UV-Vis DRS spectra of pure and K-doped cobalt oxide nanoparticles were recorded between 200 and 800 nm.

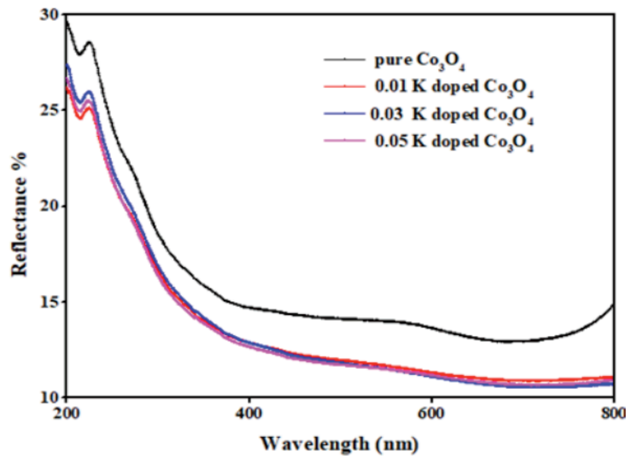

Figure 5: UV Spectrum of Co_3O_4 and K doped Co_3O_4.

The Figure **5** displays the measured reflectance of the proposed samples, which exhibits two bands of reflectance at wavelengths of 224 nm and 870 nm.

In this investigation, the tauc relation was used to calculate the band gap.

$F(R) = \frac{(1-R)^2}{2R}$ [Biswajit Choudhury *et al*., 2013]

Where R is the diffuse reflectance.

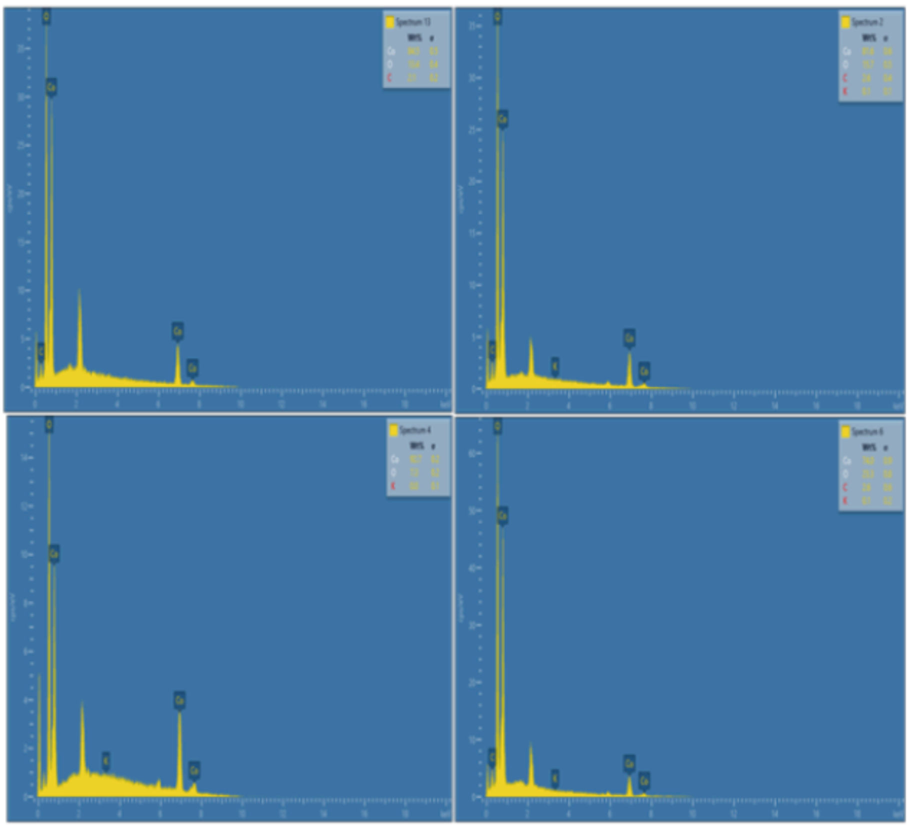

Figure 4: EDAX spectra of **a)** Pure Co_3O_4. **b)** 0.01 K doped Co_3O_4 **c)** 0.03 K doped Co_3O_4 **d)** 0.05 K doped Co_3O_4.

$[F(R)\ h\nu]^{1/n}$ where n= ½ for direct allowed and n=2 for indirect allowed transition [C. Ravi Dhas *et al.,* 2015].

The band gap can be determined by extending the linear region of the Figure **6** of $[F(R)\ h]^2$ vs photon energy. We discovered a twofold band gap for the processed samples from the Tauc plot. The double band is intended for a metal charge transfer procedure, is the justification.

$O^{2-} \rightarrow Co^{2+}$ and $O^{2-} \rightarrow Co^{3+}$ [C.Ravi Dhas *et al*., 2015] [Abdelhak Lakehal *et al*., 2018,] [Subhash Thota *et al*., 2009].

The band gap energy of the produced sample decreases as the potassium content is raised or doped [Shamsa Munir *et al*., 2016]. Following the doping of K ions, different optically active sub levels are created in the confined region of the conduction and valance band, causing the optical band gap energy to decrease [Padmini Pandey Rajnish *et al*., 2015]. The band gap energy of the K doped sample dropped as a result of the modification to the electronic structure and the quantum size impact.

Co_3O_4's optical properties are affected by a number of variables, including surface roughness, porosity, and photo-generated electron-hole carriers. The red shift phenomena may be related to the quantum effect and the absorption edge's deviation towards the longer wavelength side (222 nm to 224 nm) [Kumar, R., Sakthivel *et al*., 2019][Cheng Wang *et al*., 2011]. A spectral change towards higher wavelength is known as red shift, often referred to as bathochromic shift. The narrowing of Co_3O_4 nanoparticles' band gaps provides evidence for a quantum confinement phenomenon involving minuscule nanoparticles.

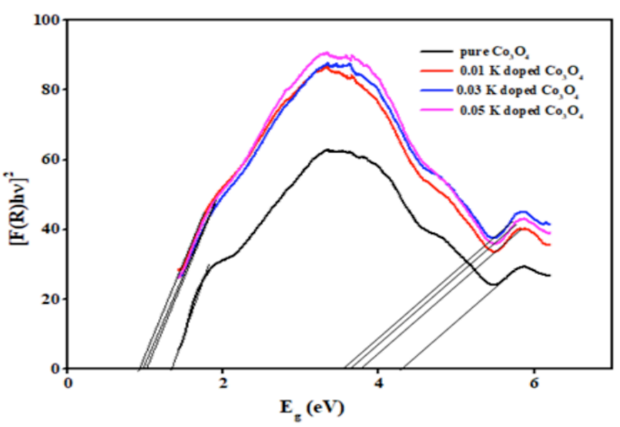

Figure 6: Tauc plot of Co_3O_4 and K doped Co_3O_4.

The graphs of h vs $[(F(R)h\nu]^2$ for K-doped Co_3O_4 are shown in Figure **6**. The K concentration causes bandgap change in Co_3O_4 that has been doped with K. Table **2** shows how the energy difference has changed as a result of the addition of K dopant. According to the methods put out by Morasae Samadi *et al*., 2016 the transition metal ion, which replaces the cation in the gap with a new electron state, interacts spin-exchangeably with its band electrons. The computed direct band gap energy decreases as K concentration rises. Given that doped Co_3O_4 has more energy levels than bare Co_3O_4, the insertion of K ions into the cobalt lattice may be the reason for the reduced band gap energy. The relevant applications of photocatalytic degradation are explained by the nanoparticles' diminishing band gap energy [Saharman Gea Suhut A *et al*., 2022] [Hesham Hamad *et al*., 2022]. [P.K. Ahluwalia and A. Kumar., 2012]. It has been noted that band gaps in the range of 1 to 2 eV are used in the manufacture of optoelectronic devices [A. Kumar and P.K. Ahluwalia., 2012]. The narrow low band gap energy of the produced samples is suitable for opto electronic applications, according to Sami Barkaoui *et al*., 2015. This material is suitable for uses based on electromagnetic devices because UV-DRS studies demonstrate that the band gap also decreases [Sharma A., 2021]. The presence of egg albumen can influence particle size and morphology and affects band gap [Liang *et al*., 2026]

Table 2: The bandgap energy of Co_3O_4 and K doped Co_3O_4

Sample	E_g in eV
Pristine	1.3 and 4.11
K 0.01	1.04 and 3.72
K 0.03	0.98 and 3.62
K 0.05	0.94 and 3.52

ELECTRICAL STUDIES

To make the electrical contact function as a parallel plate capacitor, the pure and potassium-doped Co_3O_4 nanoparticles were pelletized and electro-coated with carbon on both sides. Using an LCR meter to determine the capacitance and dissipation parameters, the dielectric constant and dielectric loss of the nanoparticles were estimated. A frequency range of 1 KHz to 1 MHz and temperatures ranging from 40 to 150 °C were used to investigate the frequency dependent dielectric characteristics of produced pure and K doped (0.01 mol, 0.03 mol, 0.05 mol) cobalt oxide nanoparticles.

Dielectric Constant

The electrical property known as the dielectric constant provides information about the atoms, ions, and their polarisation. On the basis of polarisations, it is possible to explain why the dielectric constant decreases with the applied field (ionic, orientation, and electronic). The positive ions are moved away from the negative ions as a result of ionic polarisation. In comparison to bulk materials, nanostructured materials have a high aspect ratio that results in a greater number of interfacial atoms and defects at the grain boundaries [Abraham, N. and S. Aseena., 2021], which leads to the distribution of positive and negative space charges as well as space charge polarisation. Figures **7** and **8** show how the real portion of the dielectric constant varies with frequency and temperature. From Figure **7**. With all the prepared samples we observe, as frequency rises, the peak corresponding to the Ɛ' value declines as reported by [Thoria Baeraky, 2007].

The relationship between the dielectric constant and frequency with temperature reveals that the dielectric constant lowers as frequency rises and rises as temperature rises. The fact that the generated samples have a high dielectric constant indicates that they were used to make capacitive pressure and bending sensors [N. Pereira et at 2021]. At ambient temperature, the dielectric constant is elevated due to Maxwell-Wagner interfacial polarisation. [M. Sarathbavan *et al*., 2022]. Interfacial and dipolar polarization, which depends on temperature, are what lead to the high number of Ɛ' at low frequency[J. Chand *et al*., 2011]. In The presence of egg albumen with cobalt oxide nanomaterials interface creates space charge polarisation, potentially increasing dielectric constant at low frequencies, [Maxwell-Wagner effect]. Increased temperature causes drift motion and charge carriers to be thermally activated. As a result, the dielectric constant number decreases and electron exchange contacts are intensified. Ionic and electrical polarisation start to occur in the high frequency region and this behaviour agrees with both the phenomenological model proposed by Koop and the Maxwell-Wagner polarisation model. The value of Ɛ' is larger at low frequencies because charge carriers react quickly to an externally supplied electric field. Low values of Ɛ' are produced at higher frequencies because charge carriers are unable to sustain with the fast fluctuations of applied electric field. Due to the space charge's inability to track a shift in the field, its polarization diminishes with rising frequency. Inability to track a changing electric field means that dipoles are also affected [N. Senthil Kumar, M. Ganapathy]. In the high frequency region, the dipoles will hardly be able to place themselves in the direction of the applied field, which causes the dielectric constant to decrease[M Meena *et al*.].

Using the relationship, the real portion of the dielectric constant was determined.

$$\varepsilon' = \frac{Cp \times t}{A \times \varepsilon 0}$$

Where A is the area of the sample and t is the thickness of the sample and C_p is the capacitance values

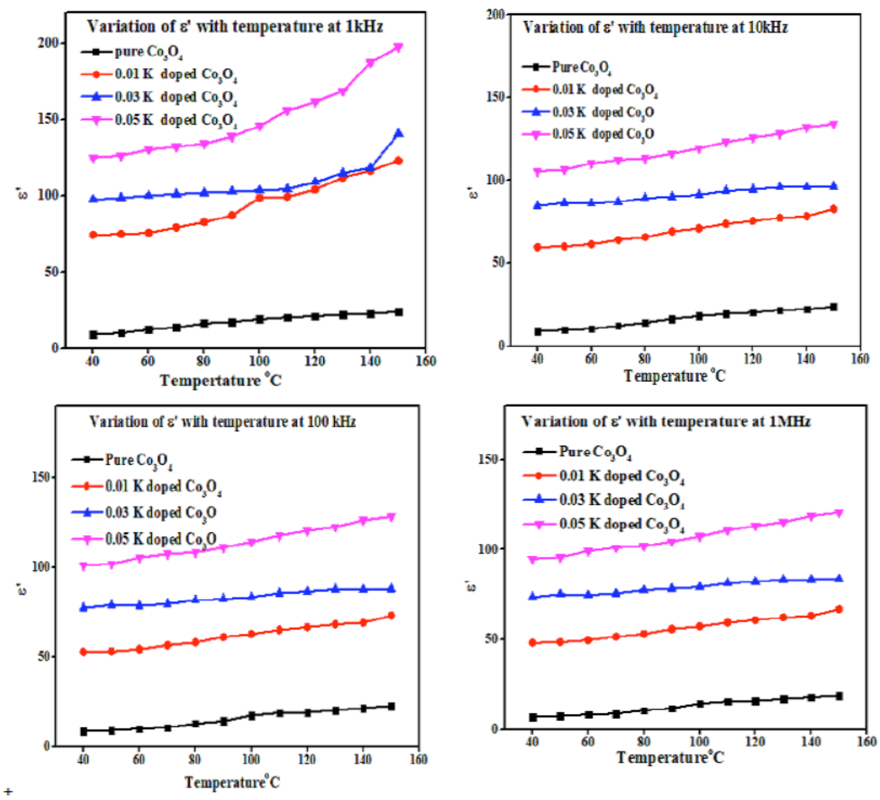

Figure 7: Variation of Ɛ' of pure and K doped Co_3O_4 with log frequency at different temperatures.

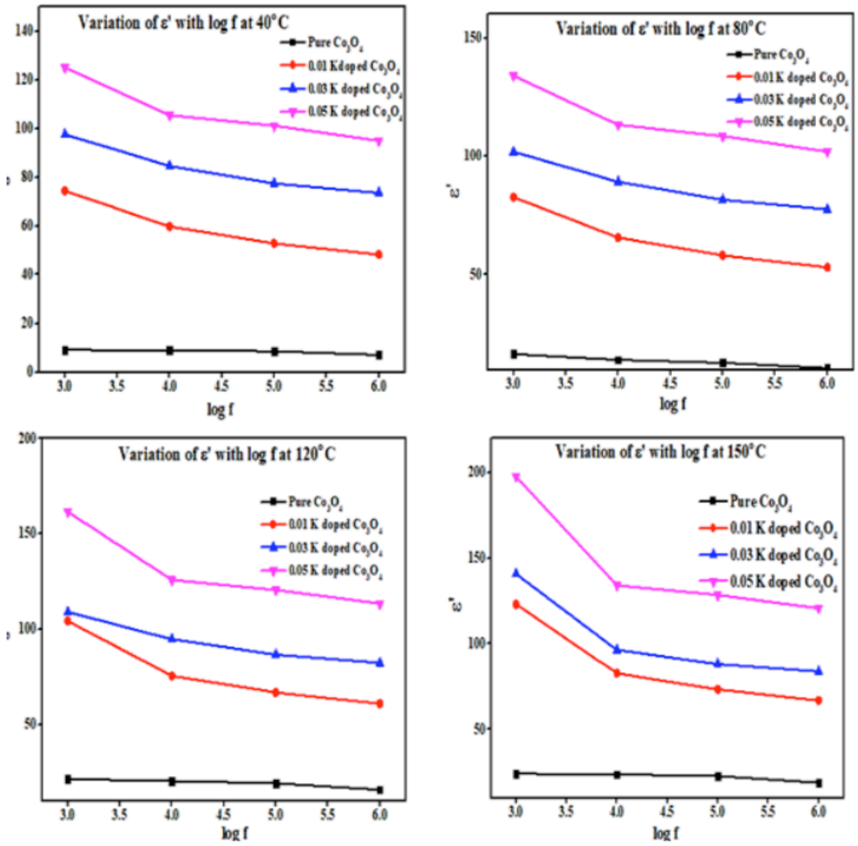

Figure 8: Variation of Ɛ' of pure and K doped Co_3O_4 with temperature at different frequencies.

And using the relationship, the imaginary portion of the dielectric constant was determined.

$$\varepsilon'' = \varepsilon' \tan\delta$$

Figures **9** and **10** show how the imaginary portion of the dielectric constant changes with frequency and temperature.

The change of dielectric loss with temperature depicted in Figure **11**. The value of the dielectric constant approaches the value of the dielectric loss in the high-frequency region. Yet, it is discovered that the dielectric constant is frequency independent in the high frequency range. Moreover, the high frequency dipoles will lose their ability to spin fully, causing their oscillation to start to lag behind the field.

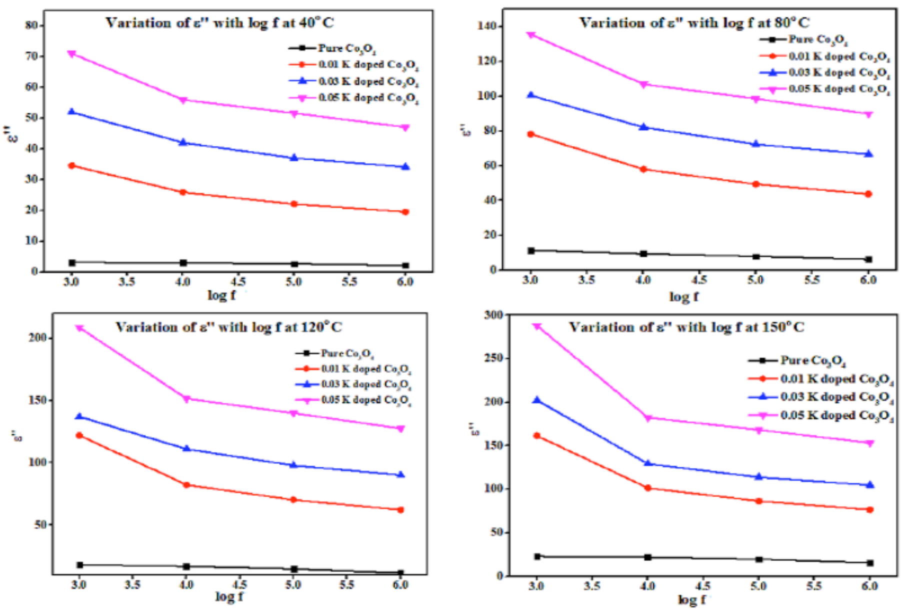

Figure 9: Variation of Ɛ'' of pure and K doped Co_3O_4 with log frequency at different temperatures.

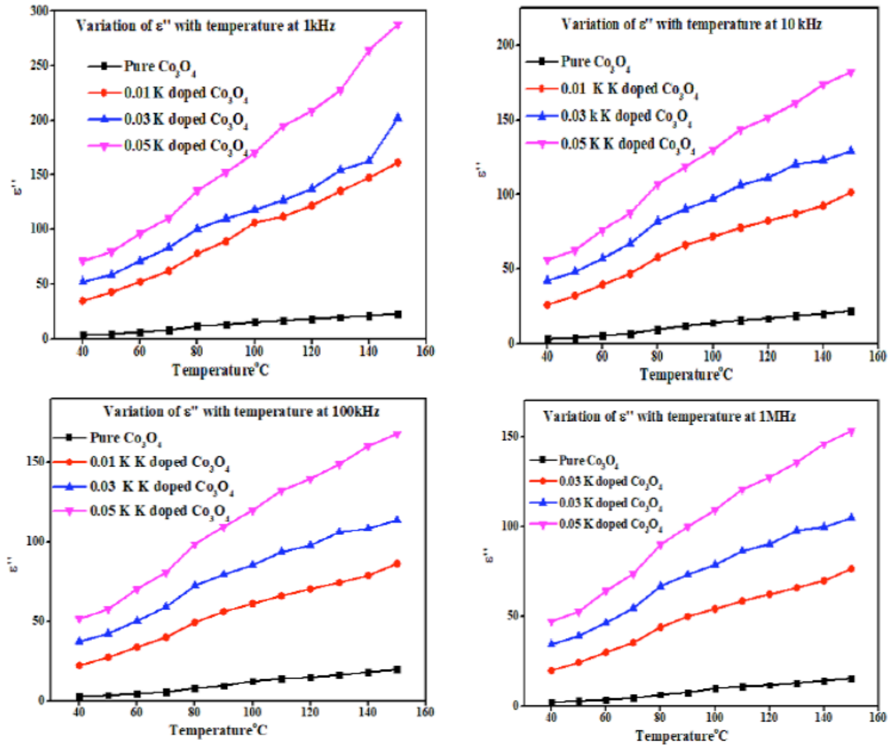

Figure 10: Variation of Ɛ'' of pure and K doped Co_3O_4 with temperature at different frequencies.

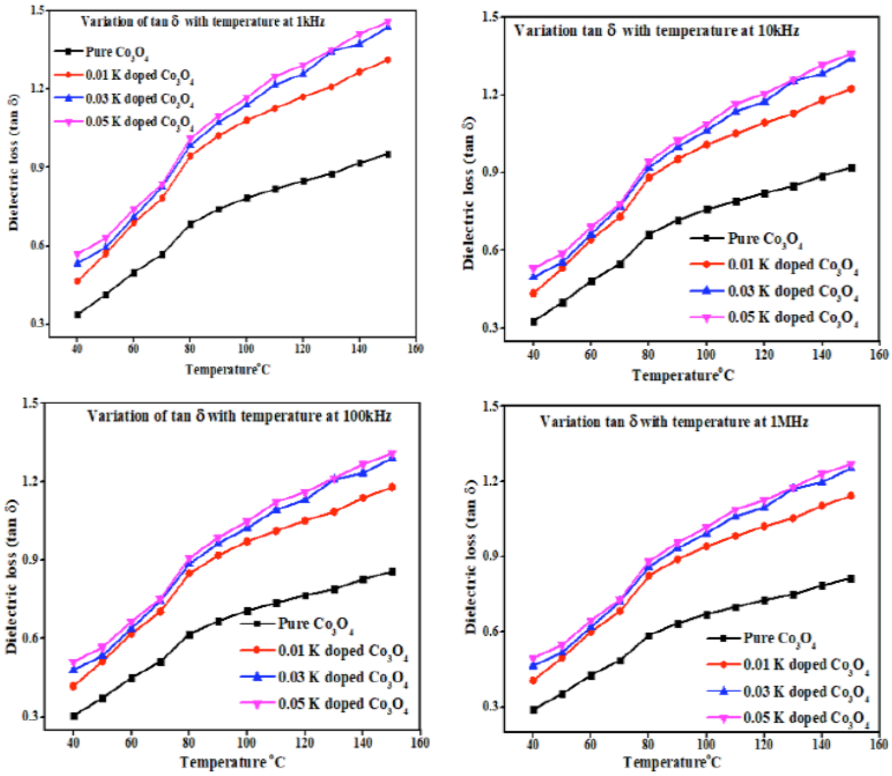

Figure 11: Variation of dielectric loss of pure and K doped Co_3O_4 with temperature at different frequencies.

As a result, the dielectric constant at high frequencies tends to be limited [T Regin Das *et al.*, 2022]. According to the plots, the electric exchange between Co and K ions, which is limited by the applied field's frequency range, results in the dielectric constant showing a declining trend with rising mole percentage and temperature. The presence of oxygen vacancies and grain boundaries as defects is crucial in deciding how a material will behave in terms of dielectric properties [Oruç, and A. Altndal., 2017].

AC Conductivity

The investigation entailed evaluating the fluctuation of the AC conductivity (AC) with frequency ($\omega=2\pi f$) for both pure and potassium-doped NPs at various temperatures ranging from 303 K to 403 K (40°C to150°C). Using the method, the electrical conductivity calculated

$$\sigma_{ac} = \omega \varepsilon' \tan\delta \varepsilon_0$$

where $\tan\delta$ is the loss tangent, ε' is the dielectric constant, and ε_0 is the vacuum dielectric constant of 8.85 × 10−12 F/m.

The change of electrical conductivity with frequency and temperature is shown in Figures **12** and **13**. According to the Figure **12** and **13**, the electrical conductivity of the Co_3O_4 samples increases as the mole percentage of dopant increases. This potassium doping enhances electrical conductivity, creates oxygen vacancies, and modifies surface chemistry for better polymer interaction. Temperature increases the conductivity in the low frequency range. The term "hopping frequency" refers to the frequency at which a conductivity transitions from being frequency dependent to being frequency independent. The hopping frequency swings towards the high frequency as the temperature rises, demonstrating the hopping of charge carriers in the material. According to the plots, the electric conductivity of the samples has a rising tendency as the mole percentage and temperature rise [N.Ch. Ramesh Babu, *et al*., 2012]. At high temperatures, the defect grows and the conductivity rises as a result of the development of electrical paths [N. Senthilkumar *et al*., 2018].

Thermal agitation and an increase in the number of charge carriers cause the total conductivity (σ) to rise with temperature [R. Sakthi Sudar Saravanan, M. Meena., 2014]. Polaron hopping is confirmed by the fact that AC electrical conductivity rises with temperature and frequency. Disordered solids, oxides, and nanocomposites all exhibit a rise in conductivity with increasing frequency.

The enhanced hopping of charge carrier phenomenon can be used to explain the increase in conductivity in the high frequency zone. The chance of charge carriers tunnelling, which is connected to the thermal oscillations of sites, can also be correlated with an increase in AC and DC conductivity. [Jamil A. Afsar *et al*., 2017]. In the low frequency region, electrical conductivity is associated with long-range mobility and grain boundaries with high resistance, whereas in the high frequency region, it is associated with short-range mobility and grains with high conductivity [Adrian Radon *et al*., 2018]. Electron hopping is the primary

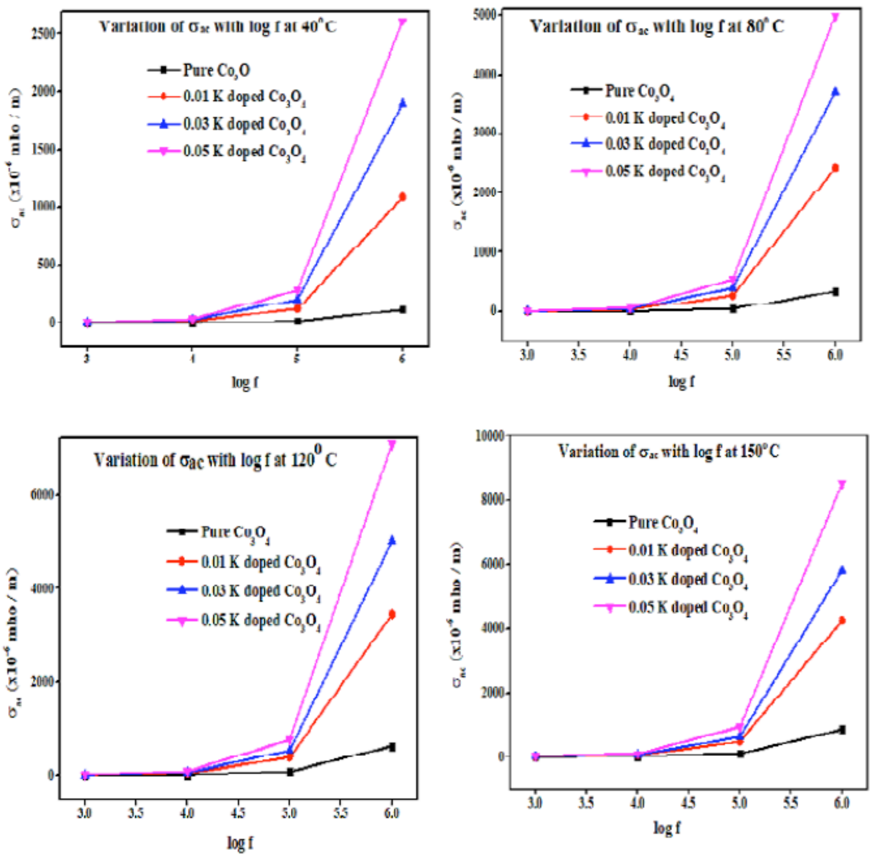

Figure 12: Variation of AC Conductivity of pure and K doped Co_3O_4 with log frequency at different temperatures.

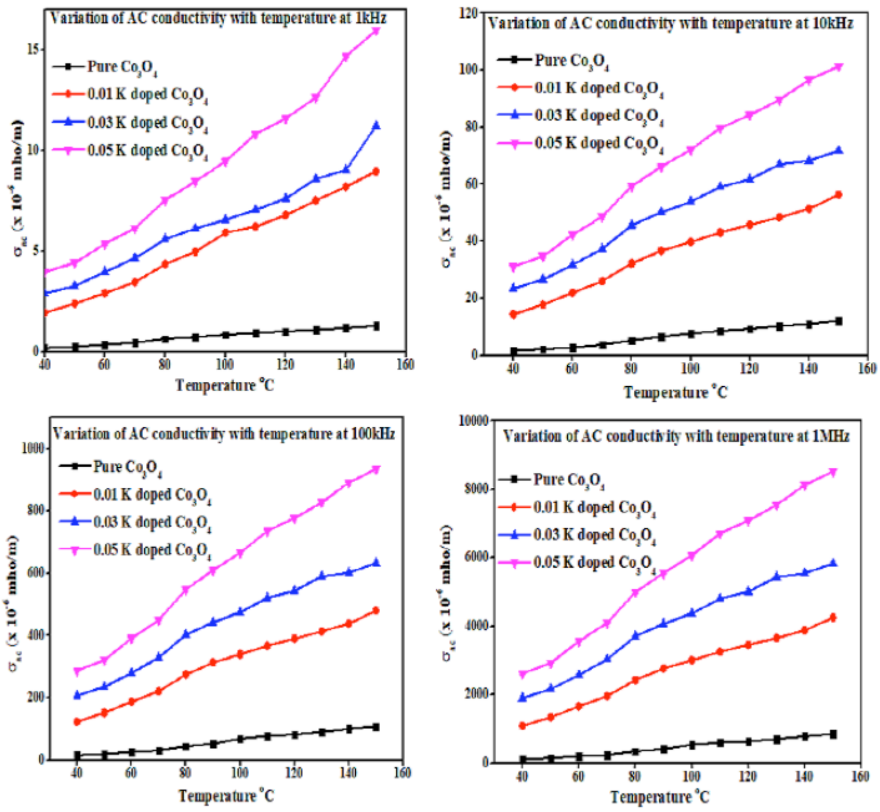

Figure 13: Variation AC conductivity of pure and K doped Co_3O_4 with temperature at different frequencies.

conduction mechanism for both high frequencies and low temperatures. [J. Kolte; Salame., 2015]

Anti Bacterial Activity

The research goal is to determine, antibacterial potential of the samples for developing antibiotic resistance. The main idea is to predict antibiotic resistance by monitoring the expansion of the inhibition zone (ZOI) around the powdered samples in order to test the antibacterial activity of the produced pure and K-doped Co_3O_4 nanoparticles, developed with egg albumen against E.coli using the aminoglycoside antibiotic class Amikacin as a control.

Inhibitory action of Pure and K doped Co_3O_4 NPs, with egg albumen

According to the picture above, the width of the inhibition zone increases as dopant concentration rises. The obtained Zone of Inhibition is greater than the previously reported biosynthesis values (Muhammad Hafeez *et al*., 2020; Rajakumar Govindasamy *et al*., 2022). Green methods were created to solve this problem because the chemicals used to fabricate NPs produce toxicity. Plant extracts rising use over the past few years is due to the existence of reducing chemicals in them since the morphology changes with the stabiliser used (Aazam and Zaheer 2016). The egg albumen is used as a binder, cum gel, and moulding material due to its water solubility and ability to combine with metal ions in solution (Dhara and Bhargava 2003). Egg albumen is therefore more effective than green leaves at enhancing antibacterial activity. Arun Singh (2022) reported with an average crystallite size of 20 nm, nanoparticles were shown to exhibit strong antibacterial activity, which is well agreed with the study of pure and K doped Co_3O_4 that has crystallite sizes of 11nm to 21nm using XRD and particle sizes of 14–20 nm. The smaller particles enhance good antibacterial activity [Yıldız, Melis, and Birol Kılıç, 2026]. The synthesised cobalt oxide nanoparticles doped with potassium and egg albumen added as a capping agent have excellent antibacterial characteristics, making them suitable for application in the construction of antibacterial dental and medical tools (Moradpoor *et al*., 2019). This egg albumin mediated synthesis represents a sustainable approach aligning principles of green chemistry while producing environmentally beneficial Biocompatible nanomaterials.

CONCLUSION

Using green synthesis, the bare and K-doped Co_3O_4 nanoparticles were effectively produced using microwave assisted hydrothermal method. The produced samples were put through structural, optical, morphological, and electrical evaluations. The green synthesis (using egg albumen) of Microwave-assisted hydrothermal technique demonstrated that the method is more convenient for the synthesis with desired nanostructures as compared to other techniques. The egg white protein albumen, the natural biopolymer has acted as shaping agent and size controller in the preparation method. The optical band gap shrinks from 1.33 eV to 0.94 eV for pure and K doped samples. Utilizing potassium doping in the egg albumen capping, the band gap was tuned in Co_3O_4. The generated nanoparticles' band gap indicates that they are appropriate for use in optoelectronic applications. With an increase in applied signal frequency, the particle's dielectric constant and dielectric loss reduce, whereas an increase in frequency causes the AC conductivity to rise. The fact that the generated samples have a high dielectric constant indicates that they were used to make capacitive pressure and bending sensors. From the aforementioned findings, it can be inferred that Co_3O_4 nanoparticles, now the bionanomaterials have outstanding characteristics that rely on morphology and surface defects in addition to particle size, band gap, and electrical properties. The developed nanoparticles with egg albumen can be modified to make them acceptable for use in the creation of antibacterial dental and healthcare equipment, a metal oxide made biocompatible synthesized using natural biopolymer and made eco-friendly.

CONFLICTS OF INTEREST

The author declared no conflicts of interest.

REFERENCES

[1] Odiachi I.J., Ize-Iyamu, O.C., Ize-Iyamu O.K., Ikechukwu, C.D., Ifijen, I.H. (2023), Systematic Review of the Synthesis of Titanium Oxide Nanoparticles via Plant Mediation Green Approach. In: TMS 2023 152nd Annual Meetng & Exihibition supplemental Proceedings. TMS 2023.The Minerals, Metals & Materials Series. Springer, Cham https://doi.org/10.1007/978-3-031-22524-6_49

[2] Guoru Li, Fengxiang Yin, Zhiping Lei, Xinran Zhao, Xiaobo He, Zhichun Li, Xiaoting Yu, Se-doped cobalt oxide nanoparticle as highly-efficient electrocatalyst for oxygen evolution reaction, International Journal of Hydrogen Energy Volume 47, Issue 1, 1 January 2022, Pages 216-227. https://doi.org/10.1016/j.ijhydene.2021.10.001

[3] Luhan Wei, Jianmin Wang, Zhen Zhao, Xi Yang, Sichen Jiao, Feng Cao, Shuai Tang, Xuefeng Zhang, Gaowu Qin, Qinghua Liang, Song Li, Co/Co_3O_4 nanoparticles embedded into thin O-doped graphitic layer as bifunctional oxygen electrocatalysts for Zn-air batteries, Chemical Engineering Journal Volume 427, 1 January 2022, 130931, https://doi.org/10.1016/j.cej.2021.130931

[4] S Gopinath, M. Mayakannan, S. Vetrivel, Structural, Optical, morphological properties of silver doped cobalt oxide nanoparticles by microwave irradiation method, Ceramic International, march 2022 pages 6103-6115. https://doi.org/10.1016/j.ceramint.2021.11.149

[5] Mushtaq Ahmad, M. A. Rafiq, and M. M. Hasan, Transport characteristics and colossal dielectric response of cadmium sulfide nanoparticles, Journal of Applied Physics 114, 133702 (2013); https://doi.org/10.1063/1.4823810

[6] P. Aji Udhaya, M. Meena, Albumen Assisted Green Synthesis of NiFe2O4 Nanoparticles and Their Physico-Chemical Properties. Science Direct, Materials Today: Proceedings 9 (2019) 528-534. https://doi.org/10.1016/j.matpr.2018.10.372

[7] Yoo, H.; Heo, K.; Ansari, M.H.R.; Cho, S. Recent Advances in Electrical Doping of 2D Semiconductor Materials: Methods, Analyses, and Applications. Nanomaterials 2021, 11, 832. https://doi.org/10.3390/nano11040832

[8] P.W. Parka, J.K. Kil1, H.H. Kunga, M.C. Kung, NO decomposition over sodium-promoted cobalt oxide, Catalysis Today 42 (1998) 51±60. https://doi.org/10.1016/S0920-5861(98)00076-5

[9] Po-Chih Chen and Sheng-Hsiung Yang, Potassium-Doped Nickel Oxide as the Hole Transport Layer for Efficient and Stable Inverted Perovskite Solar Cells, ACS Appl. Energy Mater. 2019, 2, 6705-6713. https://doi.org/10.1021/acsaem.9b01200

[10] Ai Serizawa, Facile Synthesis of Potassium-Doped Titanium Oxide Nanostructure (KTiOxs)/AlO(OH) Composites for Enhanced Photocatalytic Performance, Catalysts 2021, 11, 548. https://doi.org/10.3390/catal11050548

[11] Jie Bai, Xiaobao Xu, Ling Xu, Jin Cui, Dekang Huang, Wei Chen, Yibing Cheng, Yan Shen, and Mingkui Wang, 2013, Potassium-Doped Zinc Oxide as Photocathode Material in Dye-Sensitized Solar Cells.

[12] Batsile M. Mogudi, Phendukani Ncube, Ndzondelelo Bingwa, Naphtaly Mawila, Shitshembiso Mathebula, Reinout Meijboom, Promotion effects of alkali- and alkaline earth metals on catalytic activity of mesoporous Co_3O_4 for 4-nitrophenol reduction, Applied Catalysis B: Environmental.

[13] Hongmei An, Caitlin Kilroy, Paul J. McGinn, Combinatorial synthesis and characterization of alkali metal doped oxides for diesel soot combustion, 2004, Catalysis Today Volume 98, Issue 3, 1 December 2004, Pages 423-429. https://doi.org/10.1016/j.cattod.2004.08.006

[14] Kalai Priya, Anoop Sunny, B. Karthikeyan, D. Sastikumar, Optical, spectroscopic and fiber optic gas sensing of potassium doped α- Fe_2O_3 nanostructures, Optical Fiber Technology 58 (2020) 102304, https://doi.org/10.1016/j.yofte.2020.102304

[15] M. Jothibas, Agalya Mathivanan, Soorya Srinivasan, Investigation of molar concentration and its effects in escalated charge storage mechanism on cobalt oxide nanoparticles, Materials todays proceedings, 2023. https://doi.org/10.1016/j.matpr.2023.02.111

[16] Trang Vu Thi, Alok Kumar Rai, Jihyeon Gim, Jaekook Kim, Potassium-doped copper oxide nanoparticles synthesized by asolvothermal method as an anode material for high-performancelithium ion secondary battery, Applied Surface Science, 305 (2014) 617-625, 2014, at: https://www.researchgate.net/publication/261990941. https://doi.org/10.1016/j.apsusc.2014.03.144

[17] Muslima Zahan, Jiban Podder, Synthesis and Characterizations of Cu Doped Co_3O_4 Nanostructured Thin Films Using Spray Pyrolysis for Glucose Sensor Applications, Biointerface Research in Applied Chemistry,Volume 12, Issue 5, 2022, 6321-6335 https://doi.org/10.33263/BRIAC125.63216335

[18] Hongmei An, Paul J. McGinn, Catalytic behavior of potassium containing compounds for diesel soot combustion, Applied Catalysis B: Environmental 62 (2006) 46-56. https://doi.org/10.1016/j.apcatb.2005.06.013

[19] Biswajit Choudhury, Munmun Dey, Amarjyoti Choudhury, Defect generation, d-d transition, and band gap reduction in Cu-doped TiO_2 nanoparticles, Int. Nano Lett. 3 (25) (2013) 1-8. https://doi.org/10.1186/2228-5326-3-25

[20] C. Ravi Dhas, R. Venkatesh, K. Jothivenkatachalam, A. Nithya, B. Suji Benjamin, A. Moses Ezhil Raj, K. Jeyadheepand C. Sanjeeviraja, Visible light driven photocatalytic degradation of Rhodamine B and Direct Red using cobalt oxide nanoparticles Ceramics International, Volume 41, Issue 8, September 2015, Pages 9301-9313. https://doi.org/10.1016/j.ceramint.2015.03.238

[21] Abdelhak Lakehal, Benrabah Bedhiaf, Amar Bouaza, Hadj Benhebal, Abdel kader Ammari, Cherifa Dalache, Structural, optical and electrical properties of Nidoped Co3O4 prepared via sol-gel technique, Mater. Res. 21 (3) (2018) e20170545. https://doi.org/10.1590/1980-5373-mr-2017-0545

[22] Subhash Thota, Ashok Kumar, Jitendra Kumar, Optical, electrical and magnetic properties of Co3O4 nanocrystallites obtained by thermal decomposition of sol-gel derived oxalates, Materials Science and Engineering: B Volume 164, Issue 1, 15 August 2009, Pages 30-37. https://doi.org/10.1016/j.mseb.2009.06.002

[23] Shamsa Munir, Syed Mujtaba Shah, Hazrat Hussain, Rafaqat Ali khan, Effect of carrier concentration on the optical band gap of TiO_2 nanoparticles, Materials & Design Volume 92, 15 February 2016, Pages 64-72, https://doi.org/10.1016/j.matdes.2015.12.022

[24] Padmini Pandey Rajnish Kurchania Fozia Z. Haque, Structural, diffused reflectance and photoluminescence study of Cerium doped ZnO nanoparticles synthesized through simple sol-gel method, Optik, Volume 126, Issue 21, November 2015, Pages 3310-3315, https://doi.org/10.1016/j.ijleo.2015.06.026

[25] Kumar, R., Sakthivel, P. & Mani, P. Structural, optical, electrochemical, and antibacterial features of ZnS nanoparticles: incorporation of Sn. Appl. Phys. A 125, 543 (2019). https://doi.org/10.1007/s00339-019-2823-2

[26] Cheng Wang, Huisheng Shi, Yan Li, Synthesis and characteristics of natural zeolite supported Fe3+-TiO2 photocatalysts Applied Surface Science 257 (2011) 6873-6877. https://doi.org/10.1016/j.apsusc.2011.03.021

[27] Morasae Samadi, Mohammad Zirak, Amene Naseri, Elham Khorashadizade, Alireza Z. Moshfegh Recent progress on doped ZnO nanostructures for visible-light photocatalysis, Thin Solid Films Volume 605, 30 April 2016, Pages 2-19. https://doi.org/10.1016/j.tsf.2015.12.064

[28] Saharman Gea, Suhut A. Situmorang, Nurhaida Pasaribu, Averroes F.R. Piliang, Boy Attaurrazaq, Reka Mustika Sari, Khatarina Meldawati Pasaribu, Stergios Goutiano,2023, Facile synthesis of ZnOeAg nanocomposite supported by graphene oxide with stabilised band-gap and wider visible-light region for photocatalyst application, Journal of Materials Research and technology.

[29] Hesham Hamad, Mohamed M. Elsenety, Wagih Sadik, Abdel‑Ghafar El‑Demerdash, Adel Nashed, Amr Mostafa & Shaimaa Elyamny, 2022, The superior photocatalytic performance and DFT insights of S‑scheme CuO@TiO2 heterojunction composites for simultaneous degradation of organics, https://doi.org/10.1038/s41598-022-05981-7

[30] A. Kumar and P.K. Ahluwalia, 2012. Electronic structure of transition metal dichalcogenides monolayers 1H-MX2 (M = Mo, W; X = S, Se, Te) from ab-initio theory: new direct band gap semiconductors, Eur. Phys. J. B (2012) 85: 186. https://doi.org/10.1140/epjb/e2012-30070-x

[31] Subhash Thota, Ashok kumar, Jitendra kumar, Optical, electrical and magnetic properties of Co3O4 nanocrystallites obtained by thermal decomposition of sol-gel derived oxalates, Mater. Sci. Eng., B 164 (2009) 30-37. https://doi.org/10.1016/j.mseb.2009.06.002

[32] Abraham, N. and S. Aseena, Dielectric studies of CuO-ZnO heterojunction nanocomposites synthesized by co-precipitation method. Materials Today: Proceedings, 2021. 43: p. 3698-3700. https://doi.org/10.1016/j.matpr.2020.11.406

[33] Thoria Baeraky, A 2007, 'Microwave Measurements of Dielectric Properties of Zinc Oxide at High Temperature', Egypt. J. Solids, vol. 30, no.1,pp. 13-18. https://doi.org/10.21608/ejs.2007.149054

[34] N. Senthil Kumar, M. Ganapathy, S. Sharmila, M. Shankar, M. Vimalan, I. Vetha Potheher, ZnO/Ni (OH) 2 core-shell nanoparticles: synthesis, optical, electrical and photoacoustic property analysis J. Alloys Compd. 703, 624 (2017). https://doi.org/10.1016/j.jallcom.2017.01.323

[35] M. Meena et al Int. Journal of Engineering Research and Applications www.ijera.com ISSN: 2248-9622, Vol. 4, Issue 5(Version 5), May 2014, pp.01-07.

[36] T. Regin Das, M. Meena & I. Vetha Potheher, 2022, Enhanced UV assisted photocatalytic activity of doped and co-doped SnO_2 nanostructured material, Particulate Science and Technology. https://doi.org/10.1080/02726351.2022.2135148

[37] Oruç, Ç. and A. Altındal, Structural and dielectric properties of CuO nanoparticles. Ceramics international, 2017. 43(14): p. 10708-10714. https://doi.org/10.1016/j.ceramint.2017.05.006

[38] N.Ch. Ramesh Babu, M.A. Valente, N. Narasimha Rao, M.P.F. Graça, G. Naga Raju,M. Piasecki , I.V. Kityk ,N. Veeraiah, Low temperature dielectric dispersion and electrical conductivity studies on Fe2O3 mixed lithium yttrium silicate glasses, ∗ Journal of Non-Crystalline Solids Volume 358, Issue 23, 1 December 2012, Pages 3175-3186. https://doi.org/10.1016/j.jnoncrysol.2012.09.011

[39] N. Senthilkumar, E. Vivek, M. Shankar,M. Meena, M. Vimalan & I. Vetha Potheher, Synthesis of ZnO nanorods by one step microwave-assisted hydrothermal route for electronic device applications, J Mater Sci: Mater Electron (2018) 29:2927-2938. https://doi.org/10.1007/s10854-017-8223-5

[40] R. Sakthi Sudar Saravanan, M. Meena, D. Pukazhselvan, C. K. Mahadevan, Structural, optical and electrical characterization of Mn2+ and Cd2+ doped/co-doped PbS nanocrystals, Journal of Alloys and Compounds (2014). https://doi.org/10.1016/j.jallcom.2014.12.008

[41] Jamil, A.; Afsar, M.F.; Sher, F.; Rafiq, M.A. Temperature and composition dependent density of states extracted using overlapping large polaron tunnelling model in MnxCo1□xFe2O4 (x = 0.25, 0.5, 0.75) nanoparticles. Phys. B Condens. Matter 2017, 509, 76-83. https://doi.org/10.1016/j.physb.2017.01.005

[42] Radoń, A.; Łukowiec, D.; Kremzer, M.; Mikuła, J.; Włodarczyk, P. Electrical Conduction Mechanism and Dielectric Properties of Spherical Shaped Fe_3O_4 Nanoparticles Synthesized by Co-Precipitation Method. Materials 2018, 11, 735. https://doi.org/10.3390/ma11050735

[43] Kolte, J.; Salame, P.H.; Daryapurkar, A.S.; Gopalan, P. Impedance and AC conductivity study of nano crystalline, fine grained multiferroic bismuth ferrite (BiFeO3), synthesized by microwave sintering. AIP Adv. 2015, 5, 097164. https://doi.org/10.1063/1.4931818

[44] Maharani, N.Y., Cyrac Peter, A., Gopinath, S. et al. Growth and characterization of amino based organic nonlinear optical L-Lysine-L-Aspartate (LLA) single crystal for

electo-optic applications. J Mater Sci: Mater Electron 27, 5006-5015 (2016).
https://doi.org/10.1007/s10854-016-4387-7

[45] Sharma, A., Batoo, K.M., Aldossary, O.M. et al. Investigation of dielectric, electrical and optical properties of copper substituted Mn-Zn nanoferrites. J Mater Sci: Mater Electron 32, 313-322 (2021).
https://doi.org/10.1007/s10854-020-04782-w

[46] Tahir Rasheed, Faran Nabeel, Muhammad Bilal, Hafiz M.N. Iqbal, Biogenic synthesis and characterization of cobalt oxide nanoparticles for catalytic reduction of direct yellow-142 and methyl orange dyes, 2019, Biocatalysis and Agricultural Biotechnology Volume 19, May 2019, 101154.
https://doi.org/10.1016/j.bcab.2019.101154

[47] Ismat Bibi, Nosheen Nazar, Munawar Iqbal, Shagufta Kamal, Haq Nawaz, Shazia Nouren, Yursa Safa, Kashif Jilani, Misbah Sultan, Sadia Ata, Fariha Rehman , Mazhar Abbas, 2017, Green and eco-friendly synthesis of cobalt-oxide nanoparticle: Characterization and photo-catalytic activity, Advanced Powder Technology,
https://doi.org/10.1016/j.apt.2017.05.008

[48] Rajan Lakra, Rahul Kumar, Dhirendra Nath Thatoi, Prasanta Kumar Sahoo, Ankur Soam, 2021, Synthesis and characterization of cobalt oxide (Co_3O_4) nanoparticles, material today proceedings, Volume 41, Part 2, 2021,Pages269271.
https://doi.org/10.1016/j.matpr.2020.09.099

[49] Batsile M. Mogudi, Phendukani Ncube, Ndzondelelo, Bingwa, Naphtaly Mawila, Shitshembiso Mathebula, Reinout Meijboom, Promotion effects of alkali- and alkaline earth metals on catalytic activity of mesoporous Co_3O_4 for 4-nitrophenol reduction, 2017, Applied Catalysis B: Environmental.
https://doi.org/10.1016/j.apcatb.2017.06.045

[50] R Bhaviya Raj, M Umadevi, V Poornima Parvathi and R Parimaladevi, Effect of potassium on structural, photocatalytic and antibacterial activities of ZnO nanoparticles, 2016, Adv. Nat. Sci.: Nanosci. Nanotechnol. 7 (2016) 045008 (7pp).
https://doi.org/10.1088/2043-6262/7/4/045008

[51] Overlay panel Yan Cao, Hajar Q.Alijani MehrdadKhatami Fatemeh Bagheri-Baravati Siavash Iravani Fatemeh Sharifi, K-doped ZnO nanostructures: biosynthesis and parasiticidal application, 2021, Journal of Materials Research and Technology Volume15, November-December 2021, Pages 5445 5451.
https://doi.org/10.1016/j.jmrt.2021.10.137

[52] Po-Chih Chen and Sheng-Hsiung Yang, Potassium-Doped Nickel Oxide as the Hole Transport Layer for Efficient and Stable Inverted Perovskite Solar Cells, 2020, ACS Appl. Energy Mater. 2019, 2, 6705-6713.
https://doi.org/10.1021/acsaem.9b01200

[53] Lee, S.Y.; Matsubara, T. Numata, D. Serizawa, A. Facile Synthesis of Potassium-Doped Titanium Oxide Nanostructure (KTiOxs)/AlO(OH) Composites for Enhanced Photocatalytic Performance. Catalysts 2021, 11, 548.
https://doi.org/10.3390/catal11050548

[54] Jie Bai, Xiaobao Xu, Ling Xu, Jin Cui, Dekang Huang, Wei Chen, Yibing Cheng, Yan Shen, and Mingkui Wang, Potassium-Doped Zinc Oxide as Photocathode Material in Dye Sensitized Solar Cells, ChemSusChem 2013, 6, 622 – 629.
https://doi.org/10.1002/cssc.201200935

[55] Kimihiro Asano, Chie Ohnishi, Shinji Iwamoto, Yasushi Shioya, Masashi Inoue, Potassium-doped Co3O4 catalyst for direct decomposition of N2O, Applied Catalysis B: Environmental 78 (2008) 242-249.
https://doi.org/10.1016/j.apcatb.2007.09.016

[56] M. Sarathbavan, G. Jagadish Kumar, S. Udhayakumar, K. Kamala Bharathi, High dielectric constant, relaxor behavior and phase transitions in $Na_{0.5}Bi_{0.5}TiO_3$ nanorods, Ceramics International, Volume 48, Issue 23, Part A, 2022, Pages 34940-34947.
https://doi.org/10.1016/j.ceramint.2022.08.083

[57] N. Pereira, S. Gonçalves, J.C. Barbosa, R. Gonçalves, C.R. Tubio, J. L. Vilas-Vilela, C.M. Costa, S. Lanceros-Mendez, High dielectric constant poly(vinylidene fluoride trifluoroethylene-chlorofluoroethylene) for capacitive pressure and bending sensors. Polymer Volume 214, 1 February 2021, 123349.
https://doi.org/10.1016/j.polymer.2020.123349

[58] J. Chand, G. Kumar, P. Kumar, S.K. Sharma, M. Knobel, M. Singh, Effect of Gd3 doping on magnetic, electric and dielectric properties of $MgGdxFe_2$-xO_4 ferrites processed by solid state reaction technique. J. Alloys Compds. 509, 9638-9644 (2011).
https://doi.org/10.1016/j.jallcom.2011.07.055

[59] A. Kumar and P.K. Ahluwalia, 2012. Electronic structure of transition metal dichalcogenides monolayers 1H-MX2 (M = Mo, W; X = S, Se, Te) from ab-initio theory: new direct band gap semiconductors, Eur. Phys. J. B (2012) 85: 186.
https://doi.org/10.1140/epjb/e2012-30070-x

[60] Hmamouchi, Soufiane, Ahmed El Yacoubi, and Brahim Chafik El Idrissi. "Using egg ovalbumin to synthesize pure α-Fe_2O_3 and cobalt doped α-Fe_2O_3: structural, morphological, optical and photocatalytic properties." Heliyon 8, no. 2 (2022).
https://doi.org/10.1016/j.heliyon.2022.e08953

[61] Ao, Ran, Tao Pu, Xiujuan Yang, Siqi Zhao, Quxiu Dai, Jie Yang, Longgui Xie, Zhiying Guo, and Liping Ma. "Structure sensitivity of potassium doping on lanthanum cobalt oxide perovskite catalysts for enhancing nitric oxide oxidation." Journal of Rare Earths (2025).
https://doi.org/10.1016/j.jre.2025.06.015

[62] Chang, Yu-Shan, Jr-Wei Chen, Sheng-Yao Wang, and Yi-Chen Chen. "Valorization of egg-white byproducts into biodegradable hydrogels: Processing optimization and functional properties." Poultry Science (2026).
https://doi.org/10.1016/j.psj.2026.106472

[63] Liang, Guijiang, Wenpu Chen, Zhaojun Wang, Qiuming Chen, Maomao Zeng, Zhiyong He, Douglas Goff, and Jie Chen. "Effect of transglutaminase-mediated pre-crosslinking on the thermally induced gelation properties of soy protein and deaminated egg white protein." Food Chemistry (2026).
https://doi.org/10.1016/j.foodchem.2026.148280

[64] Abdelhamid, Hani Nasser. "Dielectric, thermal, and electrical conductivity properties of biodegradable polymer nanocomposites." (2022).
https://doi.org/10.21203/rs.3.rs-2003331/v1

[65] Ali, Maqam, Muhammad Kaleem Khosa, Awal Noor, and Sadaf Qayyum. "Synthesis, antimicrobial, antioxidant studies of thermally stable nanocomposite films doped with CoO-NPs for active food packaging applications." PLoS One 20, no. 12 (2025).
https://doi.org/10.1371/journal.pone.0338180

[66] Muhammad Hafeez, Ruzma Shaheen, Bilal Akram, Zain-ul-Abdin, Siraju Haq, Salahudin Mahsud, Shaukat Ali and Rizwan Taj Khan, 2020, Green synthesis of cobalt oxide nanoparticles for potential biological applications, Materials Research Express.
https://doi.org/10.1088/2053-1591/ab70dd

[67] Rajakumar Govindasamy, Vaishnavi Raja, Sonalika Singh, Mydhili Govindarasu, Sulthana Sabura, Kaliaperumal Rekha, V. Devi Rajeswari, Salman S. Alharthi, Manju Vaiyapuri, Rajagopal Sudarmani, S. Jesurani, Baskar Venkidasamy and Muthu Thiruvengadam, 2022, Green Synthesis and Characterization of Cobalt Oxide Nanoparticles Using Psidium guajava Leaves Extracts and Their Photocatalytic and Biological Activities, Molecules, 27, 5646.
https://doi.org/10.3390/molecules27175646

[68] Aazam, ES & Zaheer, Z,‘Growth of Ag-nanoparticles in an aqueous solution and their antimicrobial activities against Gram positive, Gram negative bacterial strains and Candida fungus’, Bioprocess and biosystems engineering, 39, pp.575-584, 2016.
https://doi.org/10.1007/s00449-016-1539-3

[69] Dhara, S & Bhargava, P, ‘A simple direct casting route to ceramic foams’, Journal of the American Ceramic Society, 86(10), pp.1645-1650, 2003.
https://doi.org/10.1111/j.1151-2916.2003.tb03534.x

[70] Arun, K Singh, 'A review on plant extract-based route for synthesis of cobalt nanoparticles: Photocatalitic, electrochemical sensing and antibacterial applications', Journal of Chemistry, 2022. https://doi.org/10.1016/j.crgsc.2022.100270

[71] Moradpoor, H, Safaei, M, Rezaei, F, Golshah, A, Jamshidy, L, Hatam, R & Abdullah, RS, 'Optimisation of cobalt oxide nanoparticles synthesis as bactericidal agents', Open access Macedonian journal of medical sciences, 7(17), p.2757, 2019. https://doi.org/10.3889/oamjms.2019.747

[72] Yıldız, Melis, and Birol Kılıç. "Effects of Green Synthesized Silver, Copper and Silver-Copper Bimetallic Nanoparticles on Foodborne Pathogens." Turkish Journal of Agriculture-Food Science and Technology 14, no. 4 (2026). https://doi.org/10.24925/turjaf.v14i4.952-957.8348

https://doi.org/10.12974/2311-8717.2026.14.05